BILINGUAL PUBLISHING CO.
Pioneer of Global Academics Since 1984

Semiconductor Science and Information Devices
https://ojs.bilpublishing.com/index.php/ssid

ARTICLE

Measurement Analysis of Specific Absorption Rate in Human Body Exposed to a Base Station Antenna by Using Finite Difference Time Domain Techniques

Hla Myo Tun[1*] Khin Kyu Kyu Win[1] Zaw Min Naing[2] Devasis Pradhan[3] Prasanna Kumar Sahu[4]

1. Department of Electronic Engineering, Yangon Technological University, Insein Township, Republic of the Union of Myanmar
2. Department of Research and Innovation, Ministry of Education, Bahan Township, Republic of the Union of Myanmar
3. Department of Electronics & Communication Engineering, Acharya Institute of Technology, Bengaluru, India
4. Department of Electrical Engineering, National Institute of Technology, Rourkela, Odisha, India

ARTICLE INFO

Article history
Received: 22 October 2021
Accepted: 18 November 2021
Published Online: 23 November 2021

Keywords:
Specific Absorption Rate (SAR)
Electromagnetic wave
Mobile basic station
Public health safety
RF waves

ABSTRACT

The system analysis of specific absorption rate (SAR) in human body exposed to a base station antenna by using finite difference time domain techniques was presented in this research works. The objectives of this work are to evaluate the knowledge and awareness about SAR among human body and mobile base station. The paper investigates the electromagnetic wave absorption inside a human body. The human body has been identified using dataset based on 2D object considering different electrical parameters. The SAR convinced inside the human body model exposed to a radiating base station antenna (BSA) has been considered for multiple numbers of carrier frequencies and input power of 20 W/carrier at GSM 900 band. The distance (R) of human body from BSA is varied in the range of 0.1 m to 5.0 m. For the number of carrier frequency equal to one and R = 0.1 m, the concentrated value of whole-body average SAR obtained by FDTD technique is found to be 0.68 W/kg which decreases either with increase of R or decrease of number of carrier frequencies. Safety distance for general public is found to be 1.5 m for number of carrier frequencies equal to one. The performance accuracy of this analysis meets the high level condition by comparing with the relevant system development in recent time.

1. Introduction

5G wireless communications system is a vital role to enhance the high speed telecommunication in modern era. The demand for huge amount of users would like to meet the specifications of 5G technology. Network Planning is the interconnection of an assortment of shards of paraphernalia to apportion resources amongst abundant users. Radio Network Planning (RNP) plays a noteworthy protagonist in the development of cellular design modeling. The Optimization practice for Network planning based on high performance antenna system could be valued of contemporary research accomplishments in academic societies. The antenna systems are very important in high performance telecommunication system and the radiation effects are affected to human body and head near the base stations due to the radio network planning and optimiza-

**Corresponding Author:*
Hla Myo Tun,
Department of Electronic Engineering, Yangon Technological University, Insein Township, Republic of the Union of Myanmar;
Email: hlamyotun@ytu.edu.mm

 https://doi.org/10.30564/ssid.v3i2.3861

tion [1]. The antenna system is very important to allocate the optimal condition for beamforming in communication system. The sustainability of 5G green network toward D2D communication with RF- energy techniques are also crucial process in green era. Heterogeneous networks had been set forth having explicit mobile sizes like macro, micro, pico and femtocells, which have confined indemnification expanses so long as contributions in apportioned expanses with virtuous sized information rates and prominence. A significant investigation on D2D communications in cellular networks. D2D communications had many advantages in contrast to conventional mobile networks can be found in [2]. The localization in 5G Green Network (5G-GN) for futuristic cellular communication is also based on the optimal arrangement of antenna system. The radiation patterns are based on the cell organization and administration in 5G green system. The productive strategies to alleviate/abuse multipath spread, the identification of view accessibility, or time synchronization plans for independent radio handsets shall be created for high performance antenna system and their radiation effects on human body. The 5G Green Network (5G-GN) is an essential enabling improvement to widespread the inevitability of information transmission from antenna system in base station. With some degree of enlargement in the number of clients and their entreaties for quality succor, energy consumption is having faith in upon to very augmentation [3,4]. The wireless cellular system [5] could provide the modern mobile telecommunication and the covering area is divided into a number of cells in a cellular system. A group of cells is being distributed over the frequency band allocated to a cellular system for an operator. An allocated base station which keeps track of the mobile phones within its range covers each cell. Each cell connects them to the telephone network and handles carry-over to the next base station when a client is leaving the coverage area [6]. The bounds of cells may diverge in size as stated by the desired capacity and geographical area to be covered [7]. In the recent digital mobile phone systems, cell sizes became much smaller and base stations are established in close of houses, schools etc., in densely populated areas. The transmitting mobile telephone BSA always radiate electromagnetic (EM) waves and those waves directly pass through human body. The body tissues absorb a significant portion of the radiated power [8]. Enormous radio wire reveal structures can fundamentally expand the accuracy of point-of-appearance-based imprisonment structures. At the same time, a number of interchanges should be picked up both at the paraphernalia space and at the sign concocting area. Precise off the bat, entirely unconventional enterprises have need of own up a restrictively extraordinary quantity of RF-to-Base-Band chains. Impenetrable radio wire constellations contemporary united coupling, unpredictable gains, and stage antiphon effects that necessitate an enhanced strategy and modification processes. The nature of human body is non-homogeneous and anisotropic. Inside the human body, absorption of EM waves at radio frequency (RF) creates standing waves, which causes localized hot spots [9]. The energy absorptions owing to localized hot spots might result in boils, drying up the fluids around eyes, brain, joints, heart, abdomen, etc. Higher level of non-ionizing radiation might destruction DNA of the living tissues [10-12]. Huge number of investigations on the harmful effects of mobile telephone BSAs are accessible in much literature but very little of that are obtainable on the effects on health [13]. The ability of the mm-Wave antenna array is in receipt of progressively momentous, predominantly for enclosed circumstances. Without a doubt, the exploitation of disinterested one anchor will document the mismanagement of a comparable structure exploited for correspondences, equally for positioning commitments. The current international safety guidelines or standards had been recognized for avoiding or limiting the potentially harmful acquaintances of human head and other body parts from the adversative biological effects due to RF exposure [14,15]. Electromagnetic Radiation is the energy propagation as electromagnetic waves or subatomic elements over and done with a vacuum, space or some material. The electromagnetic radiation is the propagation of energy from end to end an amalgamation of equivocating electric and magnetic fields; the radiation fashioned as electromagnetic fields is called electromagnetic radiation.

In this work, the measurements of SAR in Human Body Exposed to a Base Station Antenna are conducted according to the electromagnetic theory and the measured data are observed the secured location of human near the base station for telecommunication networks. The acceptable limits for permittivity of human body is 11.69, 7.98, 6.40, and 5.60 for 40, 60, 80, and 100 GHz for skin and the conductivity of human body is 31.78, 36.38, 38.38, and 39.42 for 40, 60, 80, and 100 GHz for skin. Over those values, the human would be harmful condition. The value of Max. SAR (10g ave.), W/kg is less than by comparing with the recent research works and the amount is 0.68 W/kg. It was the robust value for safety condition in real world situation. In this work, the human body was defined as the rectangular box for only simulation measurement purposes.

The paper is organized as follows. Section II presents the System Model on SAR analysis. Section III mentions the implementation procedures with appropriate flowchart. Section IV discusses on the simulation results with perfor-

  https://doi.org/10.30564/ssid.v3i2.3861

mance comparison table based on recent research works in the literature. Section V concludes the presentation of research works.

2. Background Knowledge on FDTD Techniques

The finite difference time domain (FDTD) technique is an effective and efficient scheme for analyzing the radiation effects on human body and electromagnetic simulation for time domain condition in advanced antenna system [16]. The computerized FDTD techniques for electromagnetics simulation to analyze the high power devices fabrication which was oriented to interface energy are discussed in [17]. FDTD method is a renowned preparation for the exploration of electromagnetics simulation for research purposes [18]. That preparation can elucidate a discretised Schrödinger equation in an iterative advancement. Nonetheless, the procedure offers only a second-order exact numerical clarification and essentials that the spatial grid size and time step should persuade a very limited condition in order to forfend the numerical clarification from departing. The details depiction on FDTD technique is discoursed in the following sections. The approximating the time derivatives is prearranged.

An instinctive first conjecture at approximating the time derivatives in Maxwell's Equation is

$$\nabla\times\bar{E}(t)=-\mu\frac{\partial\bar{H}(t)}{\partial t}\Rightarrow\nabla\times\bar{E}(t)\cong-\mu\frac{\bar{H}(t+\Delta t)-\bar{H}(t)}{\Delta t} \tag{1}$$

$$\nabla\times\bar{H}(t)=\varepsilon\frac{\partial\bar{E}(t)}{\partial t}\Rightarrow\nabla\times\bar{H}(t)\cong\varepsilon\frac{\bar{E}(t+\Delta t)-\bar{E}(t)}{\Delta t} \tag{2}$$

We modify the finite difference equations so that each term exists at the equivalent point in time.

$$\nabla\times\bar{E}(t)=-\mu\frac{\partial\bar{H}(t)}{\partial t}\Rightarrow\nabla\times\bar{E}(t)=-\mu\frac{\bar{H}\left(t+\frac{\Delta t}{2}\right)-\bar{H}\left(t-\frac{\Delta t}{2}\right)}{\Delta t} \tag{3}$$

$$\nabla\times\bar{H}(t)=\varepsilon\frac{\partial\bar{E}(t)}{\partial t}\Rightarrow\nabla\times\bar{H}\left(t+\frac{\Delta t}{2}\right)=\varepsilon\frac{\bar{E}(t+\Delta t)-\bar{E}(t)}{\Delta t} \tag{4}$$

These equations will acquire disorganised if we embrace interpolations.

We wobble E and H in time so that E occurs at integer time steps (0, Δt, 2Δt,...) and H occurs at half time steps (Δt/2, t+Δt/2, 2t+Δt/2,...)

$$\bar{H}\Big|_{t+\frac{\Delta t}{2}}=\bar{H}\Big|_{t-\frac{\Delta t}{2}}-\frac{\Delta t}{\mu}\left(\nabla\times\bar{E}\Big|_{t}\right) \tag{5}$$

$$\bar{E}\Big|_{t+\Delta t}=\bar{E}\Big|_{t}+\frac{\Delta t}{\varepsilon}\left(\nabla\times\bar{H}\Big|_{t+\frac{\Delta t}{2}}\right) \tag{6}$$

We will knob the spatial derivatives in $\nabla\times$ next lecture in a very comparable routine. Figure 1 shows the essential process for FDTD procedure.

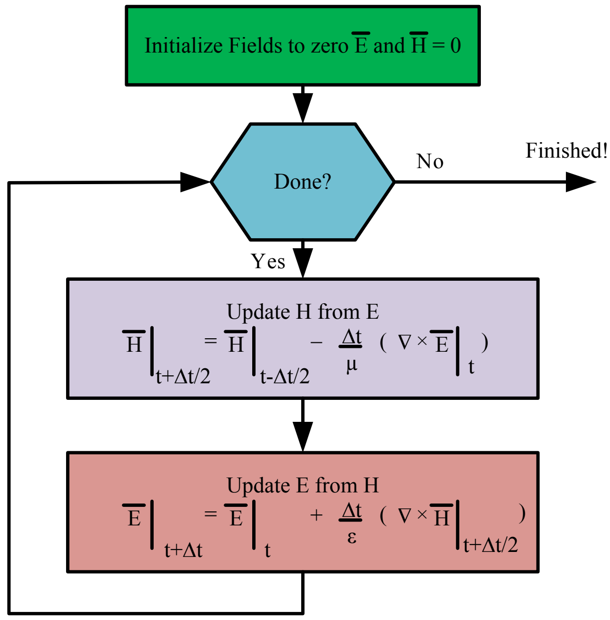

Figure 1. FDTD Procedure [18]

Assume Only Diagonal Tensors

$$\nabla\times\bar{E}=\frac{[\mu_r]}{C_0}\frac{\partial\bar{H}}{\partial t}\Rightarrow\begin{array}{l}\frac{\partial E_z}{\partial y}-\frac{\partial E_y}{\partial z}=-\frac{1}{C_0}\left[\boldsymbol{\mu_{xx}}\frac{\boldsymbol{\partial\bar{H}_x}}{\boldsymbol{\partial t}}+\mu_{xy}\frac{\partial\bar{H}_y}{\partial t}+\mu_{xz}\frac{\partial\bar{H}_z}{\partial t}\right]\\ \frac{\partial E_x}{\partial z}-\frac{\partial E_z}{\partial x}=-\frac{1}{C_0}\left[\mu_{yx}\frac{\partial\bar{H}_x}{\partial t}+\boldsymbol{\mu_{yy}}\frac{\boldsymbol{\partial\bar{H}_y}}{\boldsymbol{\partial t}}+\mu_{yz}\frac{\partial\bar{H}_z}{\partial t}\right]\\ \frac{\partial E_y}{\partial x}-\frac{\partial E_x}{\partial y}=-\frac{1}{C_0}\left[\mu_{zx}\frac{\partial\bar{H}_x}{\partial t}+\mu_{zy}\frac{\partial\bar{H}_y}{\partial t}+\boldsymbol{\mu_{zz}}\frac{\boldsymbol{\partial\bar{H}_z}}{\boldsymbol{\partial t}}\right]\end{array} \tag{7}$$

$$\nabla\times\bar{H}=\frac{[\varepsilon_r]}{C_0}\frac{\partial\bar{E}}{\partial t}\Rightarrow\begin{array}{l}\frac{\partial H_z}{\partial y}-\frac{\partial H_y}{\partial z}=+\frac{1}{C_0}\left[\boldsymbol{\varepsilon_{xx}}\frac{\boldsymbol{\partial\bar{E}_x}}{\boldsymbol{\partial t}}+\varepsilon_{xy}\frac{\partial\bar{E}_y}{\partial t}+\varepsilon_{xz}\frac{\partial\bar{E}_z}{\partial t}\right]\\ \frac{\partial H_x}{\partial z}-\frac{\partial H_z}{\partial x}=+\frac{1}{C_0}\left[\varepsilon_{yx}\frac{\partial\bar{E}_x}{\partial t}+\boldsymbol{\varepsilon_{yy}}\frac{\boldsymbol{\partial\bar{E}_y}}{\boldsymbol{\partial t}}+\varepsilon_{yz}\frac{\partial\bar{E}_z}{\partial t}\right]\\ \frac{\partial H_y}{\partial x}-\frac{\partial H_x}{\partial y}=+\frac{1}{C_0}\left[\varepsilon_{zx}\frac{\partial\bar{E}_x}{\partial t}+\varepsilon_{zy}\frac{\partial\bar{E}_y}{\partial t}+\boldsymbol{\varepsilon_{zz}}\frac{\boldsymbol{\partial\bar{E}_z}}{\boldsymbol{\partial t}}\right]\end{array} \tag{8}$$

Final Analytical Equations are as follows:

$$\begin{array}{l}\frac{\partial E_z}{\partial y}-\frac{\partial E_y}{\partial z}=-\frac{\mu_{xx}}{C_0}\left[\frac{\partial\tilde{H}_x}{\partial t}\right]\\ \frac{\partial E_x}{\partial z}-\frac{\partial E_z}{\partial x}=-\frac{\mu_{yy}}{C_0}\left[\frac{\partial\tilde{H}_y}{\partial t}\right]\\ \frac{\partial E_y}{\partial x}-\frac{\partial E_x}{\partial y}=-\frac{\mu_{zz}}{C_0}\left[\frac{\partial\tilde{H}_z}{\partial t}\right]\end{array} \tag{9}$$

$$\frac{\partial \tilde{H}_z}{\partial y}-\frac{\partial \tilde{H}_y}{\partial z}=+\frac{\varepsilon_{xx}}{C_0}\left[\frac{\partial E_x}{\partial t}\right]$$
$$\frac{\partial \tilde{H}_x}{\partial z}-\frac{\partial \tilde{H}_z}{\partial x}=+\frac{\varepsilon_{yy}}{C_0}\left[\frac{\partial E_y}{\partial t}\right] \quad (10)$$
$$\frac{\partial \tilde{H}_y}{\partial x}-\frac{\partial \tilde{H}_x}{\partial y}=+\frac{\varepsilon_{zz}}{C_0}\left[\frac{\partial E_z}{\partial t}\right]$$

The prevailing equations for verdict the finite difference condition are revealed in the succeeding section. In the beginning, the finite difference equations for H_x, H_y, and H_z for magnetic field expressions. Figure 2 to 7 show the specifics conception for magnetic field intentions from Maxwell's equations.

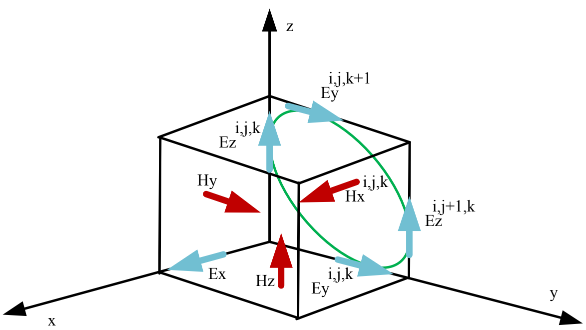

Figure 2. Equation of Finite Difference for H_x [18]

$$\frac{\partial E_z}{\partial y}-\frac{\partial E_y}{\partial z}=-\frac{\mu_{xx}}{C_0}\frac{\partial \tilde{H}_x}{\partial t} \quad (11)$$

$$\frac{E_z^{i,j+1,k}\big|_t-E_z^{i,j,k}\big|_t}{\Delta y}-\frac{E_y^{i,j,k+1}\big|_t-E_y^{i,j,k}\big|_t}{\Delta z}=-\frac{\mu_{xx}^{i,j,k}}{C_0}\frac{\tilde{H}_x^{i,j,k}\big|_{t+\frac{\Delta t}{2}}-\tilde{H}_x^{i,j,k}\big|_{t-\frac{\Delta t}{2}}}{\Delta t} \quad (12)$$

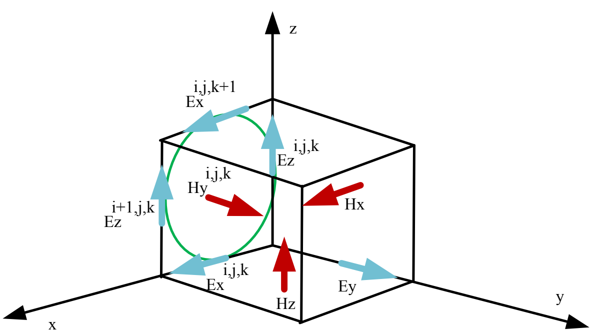

Figure 3. Equation of Finite Difference for H_y [18]

$$\frac{\partial E_x}{\partial z}-\frac{\partial E_z}{\partial x}=-\frac{\mu_{yy}}{C_0}\frac{\partial \tilde{H}_y}{\partial t} \quad (13)$$

$$\frac{E_x^{i,j,k+1}\big|_t-E_x^{i,j,k}\big|_t}{\Delta z}-\frac{E_z^{i+1,j,k}\big|_t-E_z^{i,j,k}\big|_t}{\Delta x}=-\frac{\mu_{yy}^{i,j,k}}{C_0}\frac{\tilde{H}_y^{i,j,k}\big|_{t+\frac{\Delta t}{2}}-\tilde{H}_y^{i,j,k}\big|_{t-\frac{\Delta t}{2}}}{\Delta t} \quad (14)$$

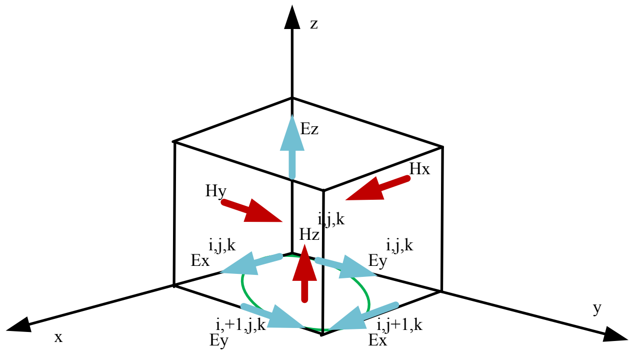

Figure 4. Equation of Finite Difference for H_z [18]

$$\frac{\partial E_y}{\partial x}-\frac{\partial E_x}{\partial y}=-\frac{\mu_{zz}}{C_0}\frac{\partial \tilde{H}_z}{\partial t} \quad (15)$$

$$\frac{E_y^{i+1,j,k}\big|_t-E_y^{i,j,k}\big|_t}{\Delta x}-\frac{E_x^{i,j+1,k}\big|_t-E_x^{i,j,k}\big|_t}{\Delta y}=-\frac{\mu_{zz}^{i,j,k}}{C_0}\frac{\tilde{H}_z^{i,j,k}\big|_{t+\frac{\Delta t}{2}}-\tilde{H}_z^{i,j,k}\big|_{t-\frac{\Delta t}{2}}}{\Delta t} \quad (16)$$

The subsequent slice is to catch the electric field expressions based on E_x, E_y, and E_z from Maxwell's Equations.

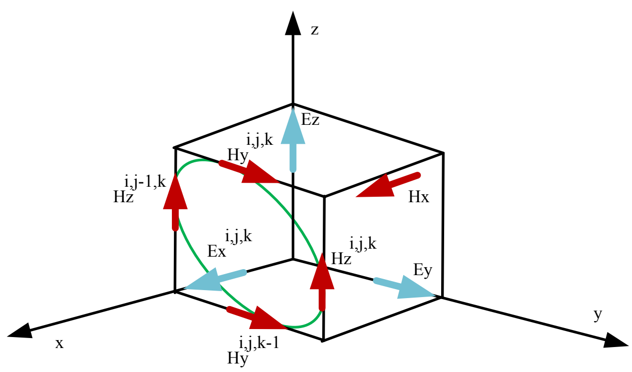

Figure 5. Equation of Finite Difference for E_x [18]

$$\frac{\partial \tilde{H}_z}{\partial y}-\frac{\partial \tilde{H}_y}{\partial z}=\frac{\varepsilon_{xx}}{C_0}\frac{\partial E_x}{\partial t} \quad (17)$$

$$\frac{\tilde{H}_z^{i,j,k}\big|_t-\tilde{H}_z^{i,j-1,k}\big|_t}{\Delta y}-\frac{\tilde{H}_y^{i,j,k}\big|_t-\tilde{H}_y^{i,j,k-1}\big|_t}{\Delta z}=\frac{\varepsilon_{xx}^{i,j,k}}{C_0}\frac{E_x^{i,j,k}\big|_{t+\Delta t}-E_x^{i,j,k}\big|_t}{\Delta t} \quad (18)$$

  https://doi.org/10.30564/ssid.v3i2.3861

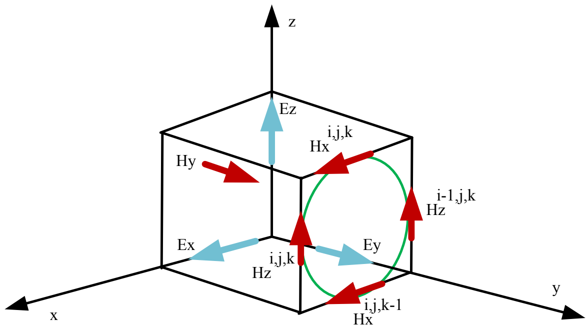

Figure 6. Equation of Finite Differenc for E_y [18]

$$\frac{\partial \tilde{H}_x}{\partial z}-\frac{\partial \tilde{H}_z}{\partial x}=\frac{\varepsilon_{yy}}{C_0}\frac{\partial E_y}{\partial t} \tag{19}$$

$$\frac{\tilde{H}_x^{i,j,k}\Big|_t-\tilde{H}_x^{i,j,k-1}\Big|_t}{\Delta z}-\frac{\tilde{H}_z^{i,j,k}\Big|_t-\tilde{H}_z^{i-1,j,k}\Big|_t}{\Delta x}=\frac{\varepsilon_{yy}^{i,j,k}}{C_0}\frac{E_y^{i,j,k}\Big|_{t+\Delta t}-E_y^{i,j,k}\Big|_t}{\Delta t} \tag{20}$$

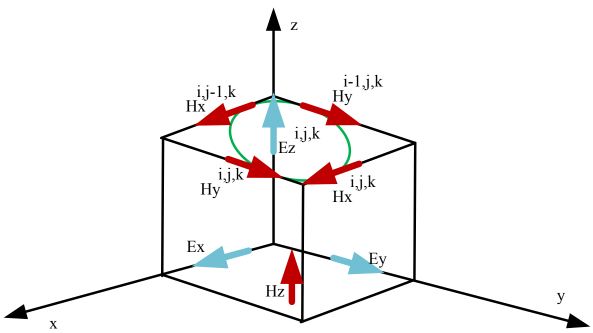

Figure 7. Equation of Finite Difference for E_z [18]

$$\frac{\partial \tilde{H}_y}{\partial x}-\frac{\partial \tilde{H}_x}{\partial y}=\frac{\varepsilon_{zz}}{C_0}\frac{\partial E_z}{\partial t} \tag{21}$$

$$\frac{\tilde{H}_y^{i,j,k}\Big|_t-\tilde{H}_y^{i-1,j,k}\Big|_t}{\Delta x}-\frac{\tilde{H}_x^{i,j,k}\Big|_t-\tilde{H}_x^{i,j-1,k}\Big|_t}{\Delta y}=\frac{\varepsilon_{zz}^{i,j,k}}{C_0}\frac{E_z^{i,j,k}\Big|_{t+\Delta t}-E_z^{i,j,k}\Big|_t}{\Delta t} \tag{22}$$

The initial conditions and the boundary conditions for using FDTD schemes shall have to be considered as follows:

- Comprehensively utilized technique for reminiscent of EM.
- No matrices are complicated in instigating.
- Rapid learning time.
- Wave dealings and coupling machineries can be premeditated.
- It is forceful, malleable, well-organized, adaptable, user friendly to elucidate Maxwell's equations in time domain condition.
- It is extensively utilized for disentangling exposed constituency smattering, electromagnetic interference (EMI), Electromagnetic compatibility (EMC).

3. System Model

The interminably intensifying diffusion of cellular phones has conveyed about an enlarged apprehension for the imaginable significance of electromagnetic radiation on human health. The dispersal of mobile phones has fetched about a greater than before disquiet for the promising values of electromagnetic radiation on the health of human being, in particular for children. In point of fact, when a cellular phone is tied down, the transmitting antenna is positioned very close to the head of user where a considerable part of the radiated power from the base station antenna is engrossed. It is problematic to experimentally measure SAR or EM field scatterings inside human body. Consequently, innumerable numerical techniques tragedy substantial roles to compute EM field constituents and SAR inside human body. FDTD scheme is one of the extensively utilized performances to act out the EM field scatterings in three dimensional configurations. The electrical properties of innumerable biological tissues, permittivity and conductivity are very significant by SAR scheming. The permittivity and conductivity hinge on frequency of the targeted system. Several parameters by SAR scheming with EMF from mobile phone are effective frequency and base station antenna power, mutual positions of the device and head intention to the device and size of human head. The FDTD technique has been utilized for voluminous applications together with conniving SAR and convinced currents in the human body and so on. In order to contemplate the effects of electromagnetic waves created from mobile phone, a planar body model has been chosen such as human body. It anticipated that a plane electromagnetic wave is incident horizontally onto the human body slabs of medium in x- direction, which electric field is in y-direction. The model consists of human body having dielectric properties for human body differ according to the frequency cogitate. There are voluminous media that have a loss term identified by conductivity. These loss term consequences in the attenuation of the propagating energy. Yet again we will jolt with the time dependent Maxwell equation, but we will transcribe them in a supplementary broad-spectrum form, which will countenance us to simulate proliferation in media that have conductivity are in Equation (1). The FDTD technique has been used for conniving SAR values for models of adults' human body, at 900 and 1800 MHz systems.

The full human body model has been constructed from rectangle shape in MATLAB which is based on reference points of a 30-year-old physically normal male weighing 80 kg and measuring 1.0m in height. To simplify the nu-

https://doi.org/10.30564/ssid.v3i2.3861

merical calculations, resolution of the human body is reduced to dimensions of 5.0 m width and 1.0 m height. The BSA used in the simulation is representative of BSAs for vertical polarization in the frequency range from 870MHz to 960 MHz. Geometry of the antenna model is reasonably close to that of the K730370 antenna and available in the literature [19,20]. Transmitted power from BSA is equal to 20 W/carrier.

Specific Absorption Rate Calculation Model

And specific absorption rate in units of (W/kg) is the utmost imperative dosimetric constraint for the estimation of the acquaintance hazard at radio and microwaves frequencies. From the congregated elucidations, the local SAR at (i,j,k) th cell inside the entire body is achieved from the succeeding equation:

$$SAR_{local} = \frac{\sigma_{head} \left| E_{base\ station}{}^{2} \right|}{2\rho_{body\ tissue}} (W/kg) \tag{23}$$

Where, $E_{base\ station}$ is the electric field (V/m) at the base station, σ_{head} = conductivity of the head (S/m), and $\rho_{body\ tissue}$ = mass density of the body tissue (kg/m^3). In this research work, the relationship between electric field, power of absorption and specific absorption rate have been appraised in life tissue of the human whole body.

Implementation

The system flowchart for analysis on Electromagnetic Radiation and SAR in Human Body Exposed to a Base Station Antenna by Using FDTD Techniques is shown in Figure 8. In this flowchart, the initialization of values for FDTD simulation on SAR calculation has to be done first. The boundary condition for FDTD was specified. The source for radiation from bans station antenna has to be created by using MATLAB. The radiation spectra on human body based on SAR was analyzed. Finally, the results of Electromagnetic Radiation and Specific Absorption Rate in Human Body Exposed to a Base Station Antenna by Using FDTD Techniques were displayed.

The FDTD time step for simulated measurement on SAR values could be chosen in arbitrarily. In this work, the significant results could be observed with the time step in the screenshot results of FDTD measurement in this paper. The color region is only mentioned for the radiation effect on human body with low level intensity (blue color) and high level intensity (yellow color) in the screenshot results in the following section.

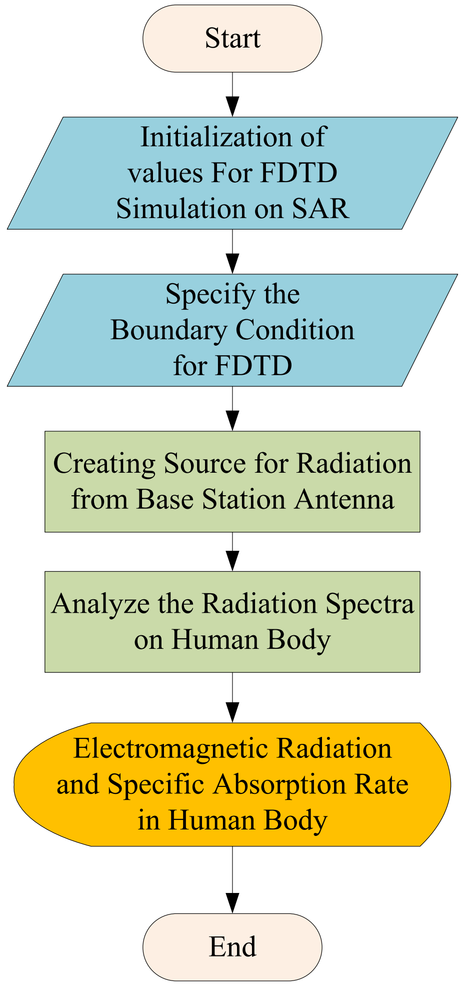

Figure 8. Flowchart of Electromagnetic Radiation and Specific Absorption Rate in Human Body Exposed to a Base Station Antenna by Using Finite Difference Time Domain Techniques

4. Results and Discussions

At first, the electromagnetic radiation with respect to FDTD time steps from 0 to 400 was implemented. According to the position of human body, the SAR on human body could be calculated by using FDTD techniques. The human body is located at 5m away from the base station antenna. And then the source of radiation will be generated the electromagnetic wave to human body. The SAR calculation was done during the FDTD calculation. Figure 9 shows the Electromagnetic Radiation w.r.t FDTD Time Step at 17. At that time step, it was the initial wave from source of radiation from the base station antenna. Figure 10 illustrates the Electromagnetic Radiation w.r.t FDTD Time Step at 106. The intensity of radiation field from the antenna was changed in that time step. Figure 11 mentions the Electromagnetic Radiation w.r.t FDTD Time Step at

https://doi.org/10.30564/ssid.v3i2.3861

182. In this time step, the radiation intensity was totally changed before reaching the human body. Figure 12 demonstrates the Electromagnetic Radiation w.r.t FDTD Time Step at 274. In this figure, the radiation wave pass through the human body and the effect would be found on the human body. Figure 13 presents the Electromagnetic Radiation w.r.t FDTD Time Step at 340. Figure 14 displays the Electromagnetic Radiation w.r.t FDTD Time Step at 400. In this figure, the intensity of radiation wave was changed for the boundary of FDTD windows. The highest intensity was on human body. Figure 15 points out the Radiation Spectra on Human Body with FDTD Simulation for SAR at 0.68 W/Kg. The SAR value was found at 0.68 W/Kg and it was the exact position of human body away from the base station antenna. The safety location is at 1.5 m from the base station antenna. This is a huge time enlargement over FDTD computations for human body models that necessitate all-embracing calculating power. In addition, our methodology is as good as in high level accuracy.

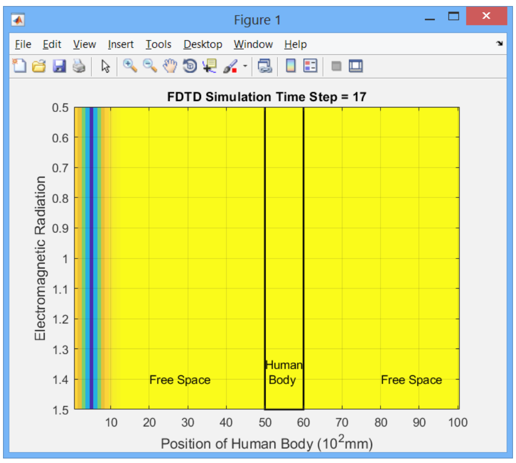

Figure 9. Electromagnetic Radiation w.r.t FDTD Time Step at 17

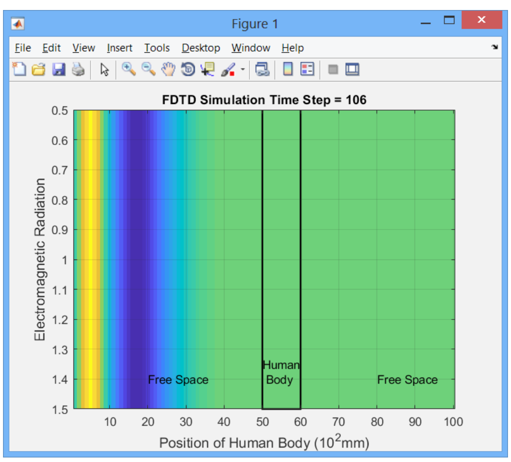

Figure 10. Electromagnetic Radiation w.r.t FDTD Time Step at 106

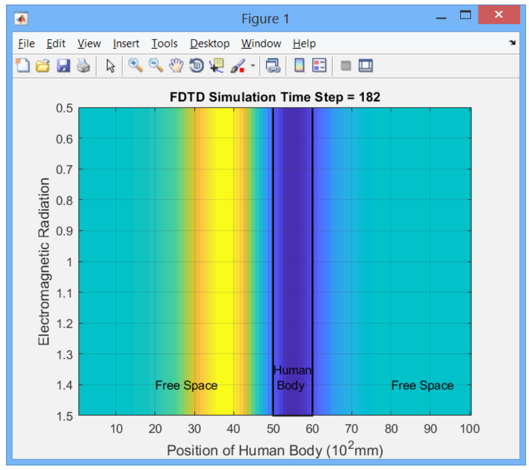

Figure 11. Electromagnetic Radiation w.r.t FDTD Time Step at 182

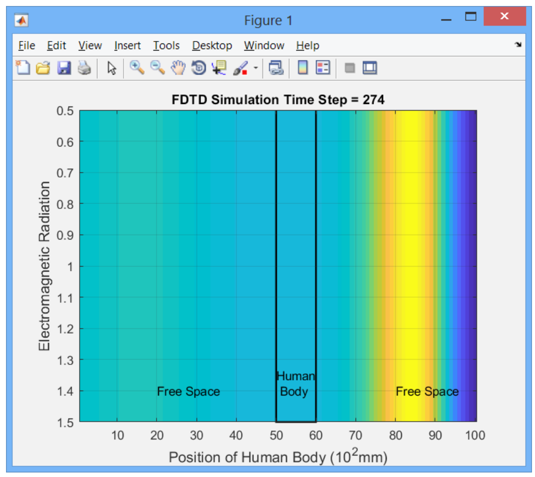

Figure 12. Electromagnetic Radiation w.r.t FDTD Time Step at 274

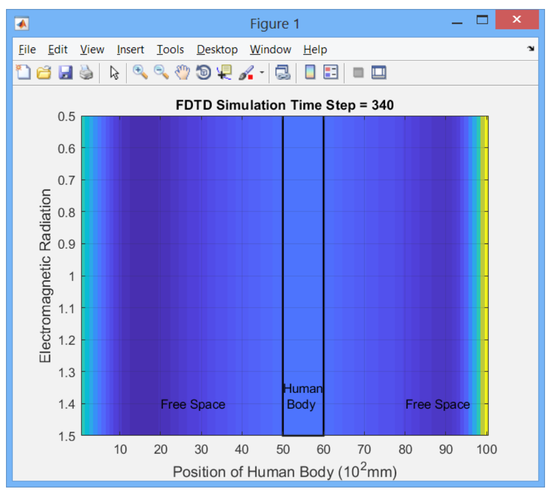

Figure 13. Electromagnetic Radiation w.r.t FDTD Time Step at 340

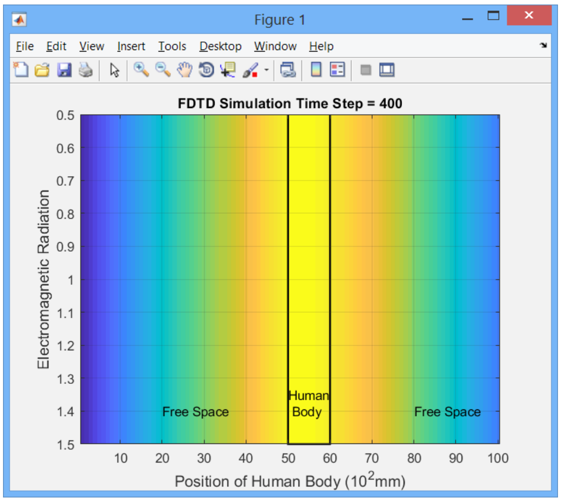

Figure 14. Electromagnetic Radiation w.r.t FDTD Time Step at 400

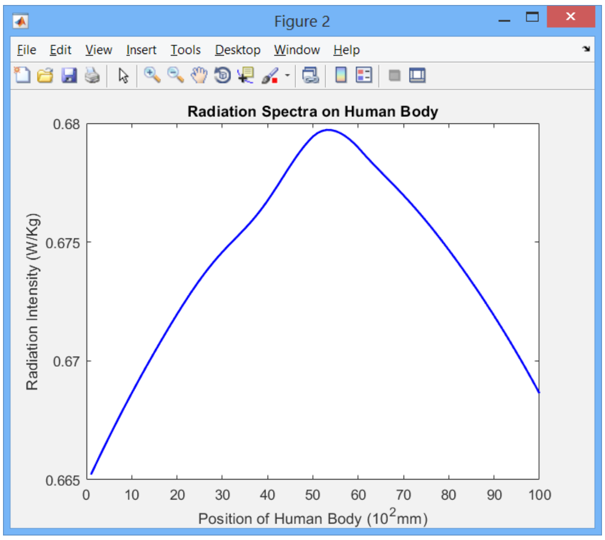

Figure 15. Radiation Spectra on Human Body with FDTD Simulation for SAR at 0.68 W/Kg

Statistic Tables for Measurement Results

Frequency and intensity of the incident EM field agrees the acquaintance bounds. The bounds are established bearing in mind the average whole body SAR not exceeding 0.4 W/kg for workers and 0.08 W/kg for general public, accompanied by experimentally strongminded inception of 4 W/kg. The development of SAR analysis on human body is summarized in Table 1 by comparing with the recent researches. There are two parameters for comparison. The first one is distance from base station and this work could provide the suitable location from base station. The distance from base station to human body is 1.5 meters. The value of Max. SAR (10g ave.), W/kg is less than in [21] and the amount is 0.68 W/kg. The details presentation is given in Table 1. In this work, we could not consider the specific location of human body. We emphasize on the whole body for analysis.

Table 1. Statistic Tables for Measurement Results on SAR Analysis for Human Boday

Research	**Contribution**	**Distance from Base Station**	**Max. SAR (10g ave.), W/kg**
This Work	Human Body	1.5 m	0.68
[21]	Human Head	Not Mentioned	0.7684
[22]	Human Head	Not Mentioned	2.12071

The SAR scattering and temperature increase have been appraised in a human body model exposed to the RF wave radiated from base station antennas. The achieved outcomes endorse the prominence of carrying out a thermal analysis in cooperation with the dosimetric one. According to the simulated measurement for SAR on human body, the secured distance is 1.5 m around the BSA because the omnidirectional antenna is used in the base station. The effect could be different in different parts of the body since the distance in terms of height converts to the angle or EMW exposed to the human body because of the electromagnetic wave theory. The result could be identical for different center frequencies of the GSM 900 band because that measurement is intended to complete the secure condition for the 5G and beyond telecommunication network in future.

5. Conclusions

The paper had been emphasized on the radiation effects on human body based on FDTD scheme at base station antenna system in 5G telecommunication environments. The FDTD analysis on absorbing boundary condition for solving a time-dependent Schrödinger equations are studied. The simulation results have been conducted by using MATLAB programming language for analysis. The SAR induced within a realistic full human body model based on human body exposed to a BSA at GSM 900 band for R in the range of 0.1 m to 5.0 m has been calculated using FDTD technique for multiple number of carrier frequencies. Transmitted power from BSA is equal to 20 W/carrier. In order to investigate the behavior of the EM field in the vicinity of the BSA distance up to 5.0 m, the distributions of the E and H field intensities in free space have been computed using MATLAB. Value of safety distance for general public from the BSA is found to be 1.5 m due to number of carrier frequencies equal to one, but this value decreases with lowering the number of carrier frequencies. On the whole, these work accompaniments the outcomes attained through FDTD schemes on convincing model of the human body, by taking to mean the outcomes from antenna theory perception. It is precisely significant

https://doi.org/10.30564/ssid.v3i2.3861

to observation that the recommendations and the standards customarily espoused in different countries only contemplate the health effects of short time of exposure.

Acknowledgement

The author would like to thank many colleagues from the Department of Electronic Engineering under the Faculty of Electrical and Computer Engineering of Yangon Technological University. This work is collaborative research with the Department of Electronics & Communication Engineering, Acharya Institute of Technology, Bengaluru, India. And also this work is a collaborative research between Yangon Technological University and University of Oulu in Finland based on the enhancement of Telecommunication Engineering Education in YTU. This work is fully supported by the government research funds of 2020-2021 academic year which is the grant no of GB/D (4)2020/4.

References

[1] Hla Myo Tun, "Radio Network Planning and Optimization for 5G Telecommunication System Based on Physical Constraints", Journal of Computer Science Research, Volume 03, Issue 01, January 2021. DOI: https://doi.org/10.30564/jcsr.v3i1.2701.

[2] D. Pradhan, P. K. Sahu, A. Dash and Hla Myo Tun, "Sustainability of 5G Green Network toward D2D Communication with RF- Energy Techniques," 2021 International Conference on Intelligent Technologies (CONIT), 2021, pp. 1-10. DOI: https://doi.org/10.1109/CONIT51480.2021.9498298.

[3] Devasis Pradhan, P.K. Sahu, Rajeswari, Hla Myo Tun, A Study of Localization in 5G Green Network (5G-GN) for Futuristic Cellular Communication, The 3rd International Conference on Communication, Devices and Computing (ICCDC 2021), India, 16-18 August 2021.

[4] Zin Mar Phyo, Tint May Nway, Khin Kyu Kyu Win, Hla Myo Tun. "Development of Microstrip Patch Antenna Design for GPS in Myanmar". American Journal of Electromagnetics and Applications. Vol. 8, No. 1, 2020, pp. 1-11. DOI: https://doi.org/10.11648/j.ajea.20200801.11.

[5] Hla Myo Tun, Aye Thandar Phyo, "Integrated WiFi/WiMAX Heterogeneous Wireless Network with Minimum Cost Flow Robust Optimization Uncertain Demand Problem", Bahria University Journal of Information & Communication Technology Vol. 3, Issue 1, pp 16-21, December 2010. Pakistan.

[6] Kundi, M. and H. P. Hutter, "Mobile phone base stations-effects on wellbeing and health," Pathophysiology, Vol. 16, 123-135, ELSEVIER, Aug. 2009.

[7] Stalling, W., Wireless Communication and Networks, Prentice Hall, 2002.

[8] Kumar, N. and G. Kumar, "Biological effects of cell tower radiation on human body," International Symposium on Microwave and Optical Technology (ISMOT), Dec. 2009, Available: http://briarcliffheights.org/bch/wp-content/uploads/2011/12/celltowerradiationeffects-100317162351-phpapp01.pdf.

[9] Ali, F., R. R. Sahoo, and S. Ray, "Study of maximum local temperature rise and hotspots distribution in a human head for GSM900 mobile phone," International Conference on Eco-friendly Computing and Communication Systems (ICECCS), 72{78, Advances in Energy Aware Computing and Communication System, Tata McGraw Hill, India, Oct. 2013, ISBN-13:978-9-35-13432-5.

[10] Lennart, H., "Epidemiological evidence for an association between use of wireless phones and tumor diseases," Pathophysiology, PATPHY-595, ELSEVIER, 2009.

[11] Blackman, C. F., et al., "Effects of ELF fields on calciumion efflux from brain tissue in vitro," Radiation Research, Vol. 92, 510-520, 1982.

[12] Lai, H. and N. P. Singh, "Melatonin and a spin-trap compound block radiofrequency electromagnetic radiation-induced DNA strand breaks in rat brain cells," Bioelectromagnetics, Vol. 18, 446-454, 1997.

[13] Kundi, M. and H. Peter, "Mobile phone base stations-effect on wellbeing and health," Pathophysiology, Vol. 16, 123-135, ELSEVIER, 2009.

[14] ICNIRP, "Guidelines for limiting exposure to time-varying electric, magnetic, and electromagnetic fields (10 kHz to 300 GHz)," Health Physics, Vol. 74, No. 4, 494-522, Apr. 1998.

[15] Council of the European Communities, "Recommendation of 12 July 1999 on the limitation of exposure of general public to electromagnetic fields (0 Hz to 300 GHz)," Official Journal of the European Communities, L.199/59-61, Jul. 30, 1999.

[16] Zin Thu Thu Lin, Hla Myo Tun. "Design and Fabrication of a Planar Inverted-F Antenna (PIFA) for LEO Satellite Application". American Journal of Electromagnetics and Applications. Vol. 8, No. 1, 2020, pp. 28-32. DOI: https://doi.org/10.11648/j.ajea.20200801.14.

[17] Phyo Sandar Win, Hsu Myat Tin Swe, Hla Myo Tun, "Computerized FDTD Method for Longitudinal Optical Phonon Energy on Semiconductor Hybrid Structure for High Power Devices Fabrication", Journal of Computer Science Research, Volume 03, Issue

02, April 2021.
DOI: https://doi.org/10.30564/jcsr.v3i2.3139.

[18] Hla Myo Tun, Thida Than, Myint Myint Than, Khin Sandar Tun, Zaw Min Naing, Maung Maung Latt, Win Khaing Moe. "Analysis on Research and Education for Electromagnetic-Applied Subjects with Finite Difference Time Domain Theory". American Journal of Electromagnetics and Applications. Vol. 6, No. 1, 2018, pp. 6-16.
DOI: https://doi.org/10.11648/j.ajea.20180601.12.

[19] Karwowski, A., "Evaluating exposure to radio-frequency emissions from base station antennas," 13th IEEE International Symposium on Personal, Indoor and Mobile Radio Communications (PIMRC), 1877-1881, Dec. 2002, Available: http://ieeexplore.ieee.org/xpl/login.jsp?tp=&arnumber=1045504&url=http%3A%2F%2Fieeexplore.ieee.org%2Fxpls%2Fabs all.jsp%3Farnumber%3D1045504.

[20] Karwowski, A., "Comparison of simple models for predicting radiofrequency fields in vicinity of base station antennas," Electronics Letters, Vol. 36, No. 10, 859-861, May 2000.

[21] M.A. Mangoud, R.A. Abd-Alhameed and P.S. Excell, Computation Of Specific Absorption Rate In The Human Body Due To Base-Station Antennas Using A Hybrid Formulation, IEEE Transactions on Electromagnetic Compatibility · June 2005.

[22] M. R. Iqbal-Faruque, N. Aisyah-Husni, Md. Ikbal-Hossain, M. Tariqul-Islam and N. Misran, "Effects of Mobile Phone Radiation onto Human Head with Variation of Holding Cheek and Tilt Positions", Journal of Applied Research and Technology, Volume 12, Issue 5, 2014, Pages 871-876, ISSN 1665-6423.
DOI: https://doi.org/10.1016/S1665-6423(14)70593-0.